



HAL
open science

Surface Charge at the Oxide/Electrolyte Interface: Toward Optimization of Electrolyte Composition for Treatment of Aluminum and Magnesium by Plasma Electrolytic Oxidation

Alexandre Nominé, Julien Martin, Cédric Noel, Gérard Henrion, Thierry Belmonte, Ilya V Bardin, Petr Lukeš

► To cite this version:

Alexandre Nominé, Julien Martin, Cédric Noel, Gérard Henrion, Thierry Belmonte, et al.. Surface Charge at the Oxide/Electrolyte Interface: Toward Optimization of Electrolyte Composition for Treatment of Aluminum and Magnesium by Plasma Electrolytic Oxidation. *Langmuir*, 2016, 32 (5), pp.1405-1409. 10.1021/acs.langmuir.5b03873 . hal-02113597

HAL Id: hal-02113597

<https://hal.science/hal-02113597>

Submitted on 6 Feb 2023

HAL is a multi-disciplinary open access archive for the deposit and dissemination of scientific research documents, whether they are published or not. The documents may come from teaching and research institutions in France or abroad, or from public or private research centers.

L'archive ouverte pluridisciplinaire **HAL**, est destinée au dépôt et à la diffusion de documents scientifiques de niveau recherche, publiés ou non, émanant des établissements d'enseignement et de recherche français ou étrangers, des laboratoires publics ou privés.

Surface charge at the oxide/electrolyte interface:
Toward optimization of electrolyte composition for
treatment of Aluminum and Magnesium by Plasma
Electrolytic Oxidation

Alexandre Nominé^{1,2}, Julien Martin¹, Cédric Noël¹, Gérard Henrion*¹, Thierry Belmonte¹,
Ilya V. Bardin³, Petr Lukeš⁴*

¹ Institut Jean Lamour – UMR 7198 CNRS – Université de Lorraine – Parc de Saurupt – 54011
Nancy, France

² The Open University – Department of Physical Science – Walton Hall MK76AA, United
Kingdom

³ National University of Science and Technology “MIS&S”, 4, Leninsky Prospekt, 119049,
Moscow, Russia

⁴ Institute of Plasma Physics, Academy of Sciences of the Czech Republic, v.v.i. Za Slovankou
3, Prague 182 00, Czech Republic

Keywords: plasma electrolytic oxidation; PEO; aluminum; magnesium; cathodic discharge; isoelectric point (IEP)

Abstract

Controlling micro-discharges in Plasma Electrolytic Oxidation is of great importance in order to optimize coating quality. The present study highlights the relationship between the polarity at which breakdown occurs and the electrolyte pH as compared with the Isoelectric point (IEP). It is found that working at a pH higher than the IEP of the grown oxide prevents the build-up of detrimental cathodic discharge. The addition of phosphates results in a shift in the IEP to a lower value and therefore promotes anodic discharges at the expense of cathodic ones.

1. Introduction

Plasma Electrolytic Oxidation (PEO) is of increasing industrial interest due to the perspectives this process offers in structure lightening and eco-friendly production. It allows fast growth (some $\mu\text{m}\cdot\text{min}^{-1}$) of crystalline oxide coatings (1-2) on the surface of light alloys (Al, Mg, Ti). Moreover, unlike anodizing, it is, a one-step process that does not require any hazardous compounds (3). The process consists in applying a sufficiently high current or voltage between a working-electrode and a counter-electrode to ensure the breakdown of the growing oxide layer in a conductive electrolyte. The as-produced micro-discharges (MDs) are essential to give access to the core material and feed the PEO-layer growth. They are responsible for the development of the porosity and roughness of the layers (4-6). It has been shown that the development of detrimental large MDs, can be limited by the use of a bipolar rather than a unipolar current (7-8) or by hybrid mode (unipolar then bipolar) (9-10) leading to significant increase in coating thickness and density and consequently an improved corrosion and wear resistance. By varying

the positive (anodic) to negative (cathodic) charge quantity ratio Q_p/Q_n , Jaspard-Mécuson et al. (11) showed that a ratio Q_p/Q_n of 0.89 led to a soft sparking regime with particularly interesting results in terms of coating thickness and homogeneity. While the importance of the cathodic half-period has been clearly established, it is interesting to note that MDs were only detected during the anodic period (i.e. when the working electrode is the anode). Considering exclusively the electrochemical processes, oxidation must take place only under anodic polarization. However, as PEO is a plasma-assisted process, it is still unclear why breakdown should occur only during the anodic half-period and not under cathodic polarization.

Previous works have shown that cathodic micro-discharges can develop not only under specific processing conditions – *e.g.* Mg alloys in NH_4F based electrolyte (12 – 13) – but also with conditions that are widely used in PEO (Mg alloys in alkaline-silicate electrolytes) (14). It has also been highlighted that cathodic MDs are detrimental to the coating growth on magnesium substrates and that they do not contribute to oxidation. It is also worth noting that cathodic MDs present different physical properties than the conventional anodic MDs; the $\text{H}\alpha$ line profiles can be fitted with a single Voigt function (i.e., only one electron density) (12) unlike results observed by Jovović et al. in the case of anodic discharges (15) and the emission intensities of different species stay relatively constant within the processing time (12) which is not what is observed in the case of anodic discharges (16). This suggests that unlike anodic discharge (16 – 17) there is likely only one type of cathodic discharge.

On the other hand, Sah et al. (18) have shown that within ranges of very high cathodic current densities (some 1000s $\text{A}\cdot\text{dm}^{-2}$) cathodic MDs can be observed. Under those conditions, cathodic MDs promote the randomisation of the anodic discharge sites, thus preventing the development of excessively large anodic discharges that are known to be detrimental to the coating

homogeneity. Therefore, predicting under which conditions cathodic MDs would occur could help to improve the process by avoiding detrimental discharges. It appears that the electrolyte composition and pH, and therefore the available charges in the electrolytic bath are the key parameters to address this issue. Hence, the present communication investigates the influence of (i) the surface charge on the grown oxide and (ii) the electrolyte composition on the breakdown regime, either anodic or cathodic or both.

2. Experimental Procedure

The process is run in an electrolytic cell equipped with glass windows. Samples are commercial Al 2024 (Cu 3.9 – 5 wt%, Mg 0.5 – 1.2 wt%, Mn 0.4 – 1.2 wt%, Fe 0.3 wt%, Si 0.5 – 1.2 wt%, Zr 0.25 wt%, Ti 0.15 wt%, Cr 0.1 wt%, Al as balance) and Mg EV31 (Nd – 2.86 wt%, Gd – 1.38 wt%, Zn – 0.25 wt%, Zr – 0.66 wt%, Mg as balance) alloys. Prior to processing, the samples are ground with water-cooled P1200 SiC paper (15.3 μm median SiC powder diameter) and rinsed successively in distilled water and ethanol. pH and composition of the electrolytes used in this study are listed in Table 1.

Table 1. Electrolyte compositions and pH

Electrolyte	Composition	pH
<i>BASE</i>	$[\text{NH}_4\text{F}] = 10 \text{ g.L}^{-1}$ (0.27 M)	6.8
<i>KOH-2</i>	<i>BASE</i> + $[\text{KOH}] = 2 \text{ g.L}^{-1}$ (0.036 M)	8.7
<i>KOH-5</i>	<i>BASE</i> + $[\text{KOH}] = 5 \text{ g.L}^{-1}$ (0.089 M)	9.2
<i>KOH-15</i>	<i>BASE</i> + $[\text{KOH}] = 15 \text{ g.L}^{-1}$ (0.268 M)	9.7
<i>KOH-20</i>	<i>BASE</i> + $[\text{KOH}] = 20 \text{ g.L}^{-1}$ (0.357 M)	12.6
<i>SILICATE</i>	<i>BASE</i> + $[\text{Na}_2\text{SiO}_3] = 2 \text{ g.L}^{-1}$ (0.016 M)	8.8
<i>PHOSPHATE</i>	<i>BASE</i> + $[\text{Na}_6\text{P}_6\text{O}_{18}] = 5 \text{ g.L}^{-1}$ (0.008 M)	8.8

Coatings are grown using a bipolar pulse current supply (Ceratron[®]), which was set to deliver a symmetrical 100 Hz quasi-square current waveform. Cathodic and anodic amplitudes are set at 8 A, (current density of 20 A.dm^{-2} delivered to the sample) leading to a ratio $Q_p/Q_n = 1$. Rise and fall times are set at $300\mu\text{s}$, off times between anodic and cathodic pulses at $100\mu\text{s}$ and hold time at $\pm 8\text{A}$ at 4.3 ms. Optical detection of MDs is performed with a photomultiplier (Hamamatsu R928) whose spectral detection covers the 185 – 900 nm range. The output signal was amplified through a 300 MHz bandwidth current amplifier (Stanford Research Systems SR445).

3. Results

3.1 Influence of surface pre-treatment

Cathodic MDs were first observed on magnesium substrates processed in BASE electrolyte (7). In this case, it was not possible to observe any cathodic MD on aluminum substrates, even though these substrates were strongly corroded. To limit corrosion and investigate the discharge behavior on aluminum substrates in BASE electrolyte, Al samples were pre-treated within the electrical conditions mentioned in Section 2. ($20 \text{ A}\cdot\text{dm}^{-2}$, 100 Hz) but in an alkaline-silicate electrolyte ($[\text{KOH}] = 0.018 \text{ M}$; $[\text{Na}_2\text{SiO}_3] = 0.0135 \text{ M}$) in order to grow oxide coatings with a thickness of 15, 30 and 45 μm . After pre-treatment, samples were PEO processed in BASE electrolyte. The evolution of light emission during one period of current is plotted in figure 1a. It clearly indicates that under the aforementioned conditions, an intense light emission due to MDs is detected during the cathodic half-period. Cathodic light emission is however detected only during the first tens of seconds of treatment (vertical dashed lines in fig. 1b); the emission occurs after longer times as the pre-coating thickness rises (20 s for 15 μm , 100 s for 45 μm). Variation of the cathodic voltage amplitude during the first two minutes of treatment shows that for cathodic discharges, a voltage peak of $\sim -180 \text{ V}$ is observed at the beginning of the process (fig. 1b) irrespective of the coating thickness. The voltage then decreases (in absolute value) at a rate which is thickness-dependent (the thinner the pre-coating, the higher the decay rate), until it reaches an asymptotic value which is proportional to the coating thickness. Interestingly, the asymptotic value is reached concomitantly with the extinction of cathodic MDs.

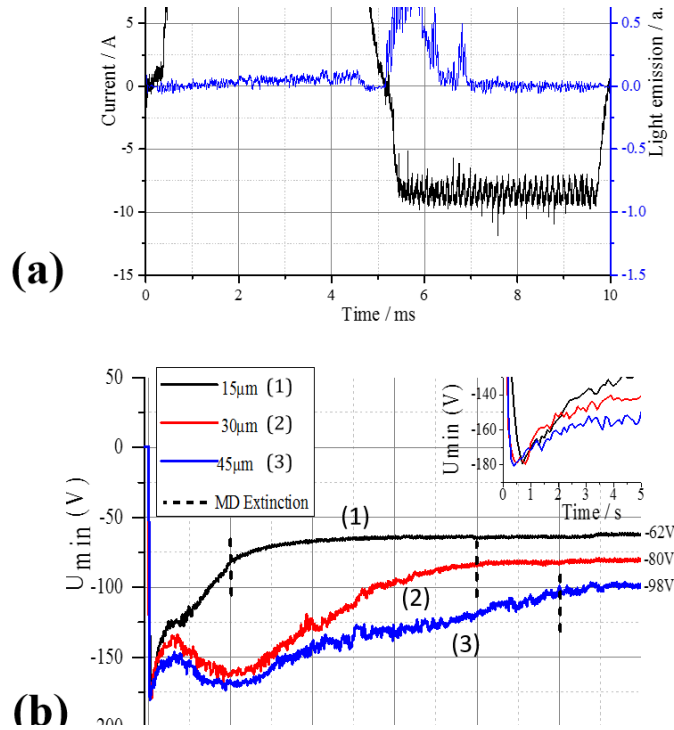


Figure 1. Variation of (a) the light emission over one current period of a pre-coated sample (coating thickness 45 μm) in BASE electrolyte and (b) the negative voltage amplitude during the first two minutes of treatments for different pre-treated samples. Vertical dashed lines indicate end of cathodic sparking.

3.2 Influence of pH

The influence of the pH was investigated by progressively adding KOH to the BASE electrolyte according to table 1. Aluminum and magnesium samples were processed within these electrolytes. Figure 2a represents the variation of the emitted light intensity over one period of current for different substrates and electrolytes. For magnesium substrates treated in an electrolyte with a low pH (KOH-2, KOH-5, KOH-15), no light emission is observed during the anodic half-period while an emission peak due to micro-discharges appears at the beginning of the cathodic polarization (fig. 2a). In the case of high pH values (KOH-20), cathodic MDs appear at the beginning of the treatment (typically after 2 minutes) and then disappear in favor of anodic micro-discharges (fig. 2a). Treatments of aluminum in KOH-20 electrolyte give rise to anodic

discharges exclusively (fig. 2a). Neither discharge nor coating growth has been observed while treating in an electrolyte with a lower KOH concentration.

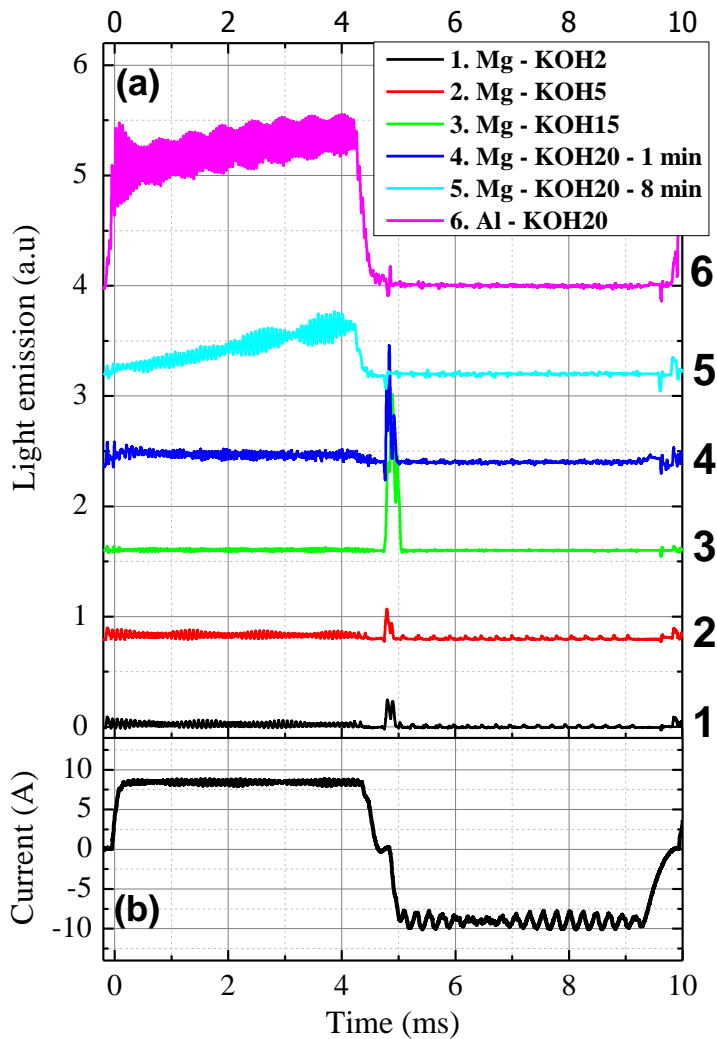


Figure 2. Chronogram of (a) the light emission and (b) the applied current over one current period for different electrolytes and substrates. Plots in fig. 2a have been shifted by 0.8 a.u to improve readability and have been recorded after 3 minutes of treatment unless otherwise specified.

3.3 Influence of electrolyte composition

Silicate- and phosphate- containing electrolytes were used to investigate the influence of the electrolyte composition. It is worth noting that both electrolytes have the same pH value (table 1). In the case of aluminum treated in SILICATE electrolyte, no discharge appeared for a bulk sample for the same reason as discussed previously. However after a pre-treatment in an alkaline-silicate electrolyte both anodic and cathodic discharges appear during one period (fig. 3a). In PHOSPHATE, only anodic discharges are observed (fig. 3a). On the other hand, in the case of a magnesium substrate, only cathodic discharges are observed in SILICATE but both anodic and cathodic discharges occur in PHOSPHATE electrolyte (fig. 3b).

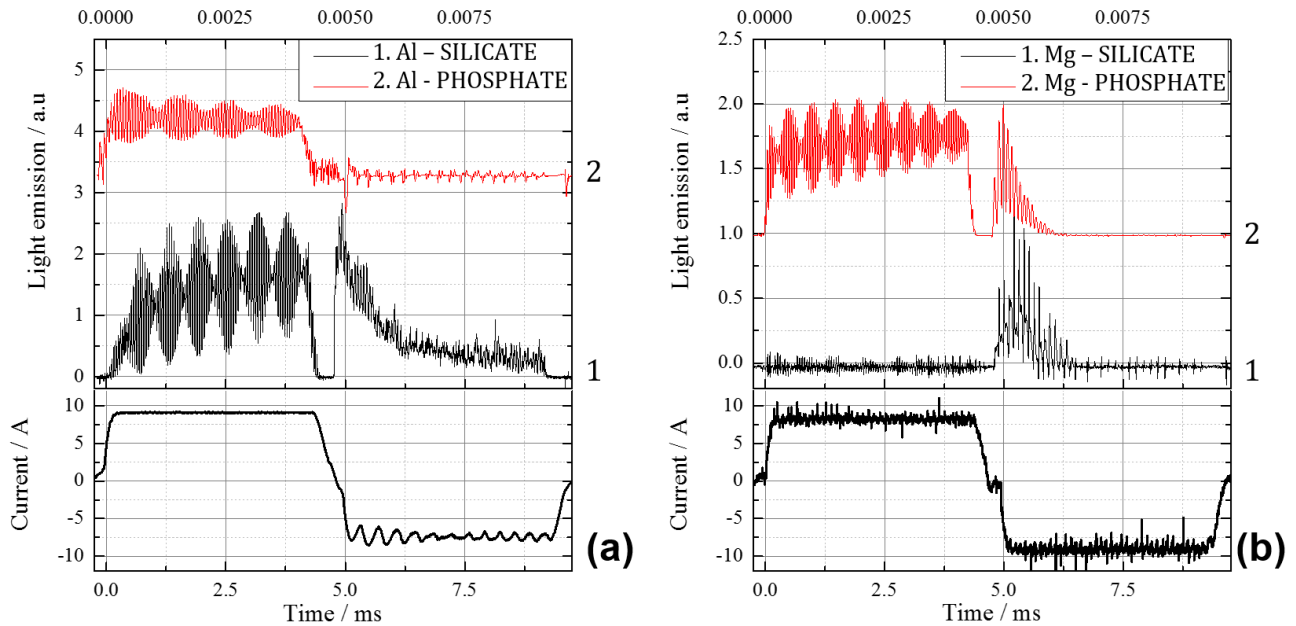


Figure 3. Evolution of light emission over one period of current for (a) aluminum and (b) magnesium substrates in SILICATE and PHOSPHATE electrolyte after 7 minutes of treatment except for the AL-SILICATE which has been recorded after 1 minute.

4. Discussion

Figure 4a shows the effect of cathodic discharges obtained on a sample previously treated in an alkaline-silicate solution (see fig 1 and § 3.1). Figure 4b shows the aspect of a sample after a 40 min treatment in the BASE electrolyte. In Figure 4a one sees that cathodic MDs strongly affect the coating which peels off at some places (see arrows) while figure 4b shows that a strong corrosion is observed in BASE electrolyte. These observations confirm that cathodic MDs are detrimental to the coating, and support the breakdown mechanism proposed in (9). It also strengthens the motivation of investigating ways to predict and prevent cathodic breakdown.

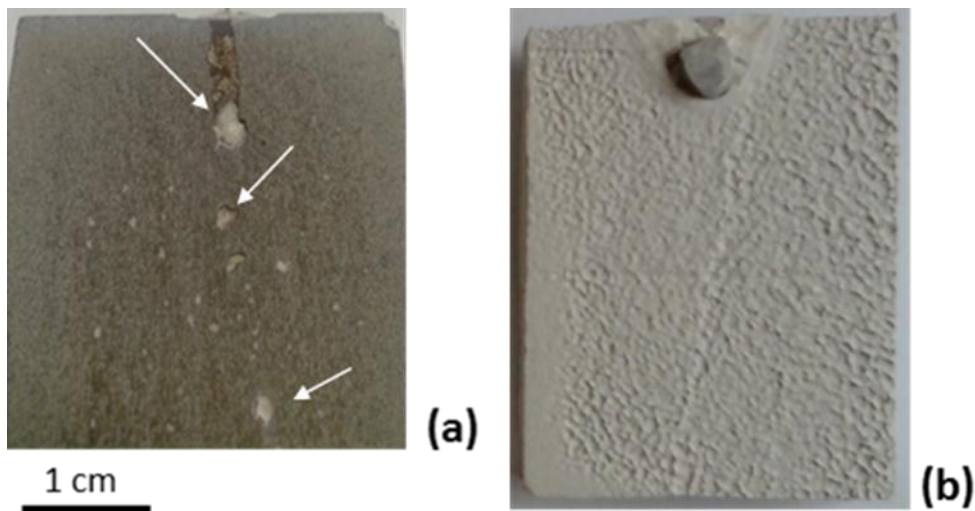


Figure 4. Photograph of (a) an aluminum sample pre-treated in an alkaline-silicate solution up to a thickness of $65\mu\text{m}$ and then treated in the BASE electrolyte (chronograms in fig 1a) and (b) a magnesium sample treated for 40 minutes in a BASE electrolyte

The presence of cathodic MDs appears to depend on both the nature of the substrate and the electrolyte composition. This suggests that electrolyte/surface interactions can promote or prevent MDs in either polarity. This was already reported by Lukeš et al. in the case of corona

discharges in aqueous electrolytes produced using metallic electrodes coated by a α - Al_2O_3 porous ceramic layer (19). According to these authors, surface charge on the oxide layer strongly affects the electric field distribution on the ceramic-coated electrode and initiation of the discharge in water. The build-up of surface charge on the oxide layer arises from acid-base dissociation of the hydrated oxide surface and accumulation of ions at the oxide/electrolyte interface. The surface charge is determined by the oxide properties and the pH of the solution. Working with a pH higher (resp. lower) than the isoelectric point (IEP) of the oxide layer promotes anodic (resp. cathodic) discharges. The IEP, also called the point of zero charge, represents the pH at which the surface charge (or zeta potential) equals zero (19 – 21). Oxide coatings, in aqueous media, become hydrated at their topmost surface and amphoteric hydroxyl groups form at the surface. These groups can catch or release a proton depending on the difference between the IEP of the material and the pH of the electrolyte. This results in either a negatively or positively charged surface. When the metallic sample is negatively biased (i.e. is cathodic) and the electrolyte pH is higher than the IEP value (negative surface charge), a large positive electric double layer (EDL) forms at the coating/electrolyte interface. The potential difference within the EDL can be estimated with the Nernst equation while the thickness of the EDL is comparable with the Debye length (see Eq. 5 and 6 in reference (19)). Typically, a pH difference of +1.5 between electrolyte pH and ceramic IEP will lead to a voltage of +100 mV within the EDL while the Debye length is between 5 and 10 nm. This leads to a local electric field as high as 100 to 200 $\text{kV}\cdot\text{cm}^{-1}$, much greater than the one applied by sample biasing (some 10s of V/cm^{-1}). This prevents cathodic breakdown (see *e.g.* (19)). Conversely, under positive bias of the electrode in an electrolyte with a pH lower than the IEP, a negative EDL forms which prevents anodic discharges. Furthermore, the surface charge of the oxide is also affected by the

specific adsorption of anions or cations present in the solution other than H^+/OH^- ions, which can induce a substantial shift in the IEP such as *e.g.*, phosphates anions in the case of Al_2O_3 ($\Delta IEP = -4$) (20). This approach is valid whatever the breakdown mechanism considered (breakdown of the liquid electrolyte, of the ceramic coating, of gas bubble in pores...) since the presence or absence of an EDL will influence the charge accumulation that is necessary for breakdown of any kind.

Table 2 sums up the results obtained in this work and from other works, in terms of electrolyte pH and the resulting breakdown regime. Isoelectric points have been taken from Parks (21) and Kosmulski (20) data bases. The IEP of MgO was determined by the classical electrokinetic method while in the case of Al_2O_3 a broad spectra of value was found depending on the crystallographic phase, the measurement method and the salt used. Since PEO coatings are composed of α - and γ - Al_2O_3 we could establish that the IEP is between 8 and 9.5. The majority of the IEP measurement were done by classical electrokinetics though some results were obtained by CIP (common intersection point) or using the electroacoustic method (further details can be found elsewhere (20)).

Table 2. Dependence of the breakdown regime on the type of substrate and on the electrolyte pH and composition. (C and A types of MD stand for cathodic and anodic respectively)

N°	Substrate	Electrolyte	pH	IEP	MD type	Ref.
1	Mg	<i>BASE</i>	6.8	12.4 ± 0.3	C	(12)
2	Al	<i>BASE</i>	6.8	8 – 9.5	C	Fig. 1
3	Mg	<i>KOH-20</i>	12.6	12.4 ± 0.3	C then A	Fig. 2
4	Al	<i>KOH-20</i>	12.6	8 – 9.5	A	Fig. 2
5	Mg	<i>KOH-5</i>	9.15	12.4 ± 0.3	C	Fig. 2
6	Mg	<i>SILICATE</i>	8.8	12.4 ± 0.3	C	Fig. 3
7	Mg	<i>PHOSPHATE</i>	8.8	?	C & A	Fig. 3
8	Al	<i>SILICATE</i>	8.8	8 – 9.5	C & A	Fig. 3
9	Al	<i>PHOSPHATE</i>	8.8	5.0	A	Fig. 3
10	Mg	KOH+Na ₂ SiO ₃	12.6	12.4 ± 0.3	C & A	(14)
11	Mg	Na ₂ SiO ₃ + Na ₄ P ₂ O ₇ ·10H ₂ O	12.5	?	A	(22)
12	Al	KOH + Na ₂ SiO ₃	12.5	8 – 9.5	C & A	(18)
13	Al	KOH + Na ₂ SiO ₃ + Na ₄ P ₂ O ₇	12	5	A	(23)

It clearly appears that the breakdown regime depends on whether the electrolyte pH is above or below the material IEP. In other words, working at a pH higher than the IEP promotes anodic breakdown and prevents the cathodic one. In conditions 7, 8 and 10, the two discharge regimes occur concomitantly. In conditions 8 and 10, the electrolyte pH is very close to the oxide IEP. Consequently, the pH-dependant surface potential is very small, decreasing the shielding efficiency. Therefore, breakdown can occur with either polarity. In conditions 7 and 11, the issue is that the value of the IEP of MgO in phosphate is unknown. However if we assume that phosphate induces a similar IEP shift on MgO as on Al₂O₃, the IEP of MgO in phosphate should be around pH 8.5. Assuming so, it is not surprising that only anodic discharges appear in condition 11 while the coexistence of cathodic and anodic discharges (condition 7) could be explained just as for conditions 8 and 10. One should point out the beneficial effect of phosphate that shifts the IEP to lower values and thus extends the range of pH for which cathodic MDs are inhibited. The same reasoning holds for condition 3. In that case however, it is likely that the morphology and structure of the growing layer slightly modify the IEP towards higher values, which would explain that cathodic discharges appear first and anodic ones after a few minutes of treatment. In condition 12, the presence of cathodic discharge is likely due to the very high current imposed (some 1000s of A.dm⁻² while 20 – 65 A.dm⁻² were used in other conditions). Hence, the surface charge is likely to be insufficient to shield from such a high current and discharges can form within both anodic and cathodic bias voltages.

5. Conclusion

To conclude, synchronized measurements of micro-discharges during PEO processing of various samples within different electrolyte allow the following conclusions to be drawn:

- Detrimental cathodic breakdown can be avoided by adjusting the electrolyte pH to values higher than the isoelectric point of the growing oxide in the same electrolyte. This is due to the double layer that forms at the surface and which lowers the electric field across the oxide layer
- Adding phosphate compounds in the electrolyte shifts the IEP to lower values. Besides avoiding the cathodic discharging, this allows a wider range of pH values to be used for which only anodic breakdown occurs.

AUTHOR INFORMATION

Corresponding Authors

* Dr. Alexandre Nominé, mail: alexandre.nomine@open.ac.uk

* Dr. Gérard Henrion, mail: gerard.henrion@univ-lorraine.fr

Funding Sources

We greatly acknowledge the Conseil Régional de Lorraine for granting A. Nominé's PhD work under decision 11CP-769. This work was carried out within the framework of the COST TD1208 network.

ACKNOWLEDGMENT

The authors are grateful to Prof. T.W Clyne and Prof. N.StJ. Braithwaite for useful discussion and Pr. E. McRae for careful proof reading and supervising English writing

ABBREVIATIONS

PEO plasma electrolytic oxidation; IEP isoelectric point; MD micro-discharge; EDL electric double layer

REFERENCES

- (1) K. Tillous, T. Toll-Duchanoy, E. Bauer-Grosse, L. Hericher, et G. Geandier, Microstructure and phase composition of microarc oxidation surface layers formed on aluminium and its alloys 2214-T6 and 7050-T74, *Surf. Coat. Technol.*, **2009**, 203, 2969–2973
- (2) Sundararajan G.; Rama Krishna L.; Mechanisms underlying the formation of thick alumina coatings through the MAO coating technology, *Surf. Coat. Technol.*, **2003**, 167, 269-277

- (3) Yerokhin, A. L.; Nie, X.; Leyland, A.; Matthews, A.; Dowey, S. J. Plasma electrolysis for surface engineering, *Surf. Coat. Technol.* **1999**, 122, 73-93.
- (4) Moon S.; Arrabal R.; Matykina E.; 3-Dimensional structures of open-pores in PEO films on AZ31 Mg alloy, *Mat. Lett.* **2015**, 161, 439–441
- (5) Curran J. A.; Clyne T. W.; Porosity in plasma electrolytic oxide coatings, *Acta Mater.*, **2006**, 54, 1985–1993.
- (6) Tillous E.K.; Toll-Duchanoy T.; Bauer-Grosse E.; Microstructure and 3D microtomographic characterization of porosity of MAO surface layers formed on aluminium and 2214-T6 alloy, *Surf. Coat. Technol.* **2009** 203 1850–1855
- (7) R. O. Hussein, P. Zhang, X. Nie, Y. Xia, et D. O. Northwood, The effect of current mode and discharge type on the corrosion resistance of plasma electrolytic oxidation (PEO) coated magnesium alloy AJ62 , *Surf. Coat. Technol.* **2011** 206 1990- 1997
- (8) A. L. Yerokhin, L. O. Snizhko, N. L. Gurevina, A. Leyland, A. Pilkington, et A. Matthews, Spatial characteristics of discharge phenomena in plasma electrolytic oxidation of aluminium alloy , *Surf. Coat. Technol.* **2004** 177 779- 783
- (9) R. O. Hussein, D. O. Northwood, J. F. Su, et X. Nie, A study of the interactive effects of hybrid current modes on the tribological properties of a PEO (plasma electrolytic oxidation) coated AM60B Mg-alloy , *Surf. Coat. Technol.* **2013** 215 421- 430
- (10) R. O. Hussein, D. O. Northwood, et X. Nie, The effect of processing parameters and substrate composition on the corrosion resistance of plasma electrolytic oxidation (PEO) coated magnesium alloys , *Surf. Coat. Technol.*, **2013** 237 357- 368

- (11) F. Jaspard-Mécuson, T. Czerwicz, G. Henrion, T. Belmonte, L. Dujardin, A. Viola, et J. Beauvir, Tailored aluminium oxide layers by bipolar current adjustment in the Plasma Electrolytic Oxidation (PEO) process , *Surf. Coat. Technol.* **2007** 201 8677- 8682
- (12) Nomine, A.; Martin, J.; Noel, C.; Henrion, G.; Belmonte, T.; Bardin, I. V.; Kovalev, V. L.; Rakoch, A. G. The evidence of cathodic micro-discharges during plasma electrolytic oxidation process, *Appl. Phys. Lett.* **2014**, 104, 081603.
- (13) Rakoch, A. G.; Gladkova, A. A.; Linn, Z.; Strekalina, D. M. The evidence of cathodic micro-discharges during plasma electrolytic oxidation of light metallic alloys and micro-discharge intensity depending on pH of the electrolyte, *Surf. Coat. Technol.* **2015**, 269, 138-144.
- (14) Nomine, A.; Martin, J.; Henrion, G.; Belmonte, T. Effect of cathodic micro-discharges on oxide growth during plasma electrolytic oxidation (PEO), *Surf. Coat. Technol.* **2015**, 269, 131–137.
- (15) J. Jovovic, S. Stojadinovic, N. M. Sisovic, et N. Konjevic, Spectroscopic study of plasma during electrolytic oxidation of magnesium- and aluminium-alloy, *J. Quant. Spectrosc. Radiat. Transf.*, **2012**, 113, 1928- 1937.
- (16) R. O. Hussein, X. Nie, D. O. Northwood, A. Yerokhin, et A. Matthews, Spectroscopic study of electrolytic plasma and discharging behaviour during the plasma electrolytic oxidation (PEO) process, *J. Phys. -Appl. Phys.*, **2010**, 43, 105203.

- (17) Y. Cheng, Z. Xue, Q. Wang, X.-Q. Wu, E. Matykina, P. Skeldon, et G. E. Thompson, New findings on properties of plasma electrolytic oxidation coatings from study of an Al–Cu–Li alloy, *Electrochimica Acta*, **2013**, 107, 358- 378.
- (18) Sah, S. P.; Tsuji, E.; Aoki, Y.; Habazaki, H. Cathodic pulse breakdown of anodic films on aluminium in alkaline silicate electrolyte - Understanding the role of cathodic half-cycle in AC plasma electrolytic oxidation, *Corros. Sci.* **2012**, 55, 90- 96.
- (19) Lukes, P.; Clupek, M.; Babicky, V.; Sunka, P. The Role of Surface Chemistry at Ceramic/Electrolyte Interfaces in the Generation of Pulsed Corona Discharges in Water Using Porous Ceramic-Coated Rod Electrodes, *Plasma Process. Polym.* **2009**, 6, 719- 728.
- (20) Kosmulski, M. pH-dependent surface charging and points of zero charge. IV. Update and new approach, *J. Colloid Interface Sci.* **2009**, 337, 439- 448.
- (21) Parks, G. Isoelectric Points of Solid Oxides Solid Hydroxides and Aqueous Hydroxo Complex Systems, *Chem. Rev.* **1965**, 65, 177- 198.
- (22) Arrabal, R.; Matykina, E.; Hashimoto, T.; Skeldon, P.; Thompson, G. E. Characterization of AC PEO coatings on magnesium alloys, *Surf. Coat. Technol.* **2009**, 203, 2207–2220.
- (23) Dunleavy, C. S.; Golosnoy, I. O.; Curran, J. A.; Clyne T. W. Characterisation of discharge events during plasma electrolytic oxidation, *Surf. Coat. Technol.* **2009**, 203, 3410-3419.

TOC GRAPHIC

